

## Understanding the properties of processed polyamide 11

Katalee Jariyavidyanont, Jason L. Williams, Alicyn M. Rhoades, Ines Kühnert, Walter Focke, and René Androsch

*Calculating different cooling rates for injection-molded polyamide 11 enables successful prediction of crystal polymorph details in actual molded parts.*

Polyamide 11 (PA11) is an increasingly important industrial polymer. Previous studies have shown that PA11 can develop different crystal polymorphs, depending on the cooling rate and crystallization temperature.<sup>1–11</sup> This has implications for injection molding, extrusion, and other polymer processing techniques where bulk properties ultimately result from the aggregate microstructure. However, until now, little has been known about the extent to which the microstructure of injection-molded PA11 depends on the processing conditions. We simulated flow across the cross section of a molded tensile specimen to predict a cooling-rate profile. We then applied a simple thermal analysis to predict the microstructure of the finished part.<sup>12</sup>

Fast scanning calorimetry has shown that PA11 can only crystallize from the melt if the cooling rate is slower than  $600\text{Ks}^{-1}$ .<sup>13</sup> Faster cooling rates yield amorphous PA11 because the material does not have time to organize before solidification. Rates near  $600\text{Ks}^{-1}$  will yield the pseudohexagonal, less-ordered, smectic-like  $\delta'$ -mesophase. If the cooling rate is between 100 and  $600\text{Ks}^{-1}$ , PA11 forms pseudohexagonal  $\delta$ -crystals. Cooling rates that are slower than  $100\text{Ks}^{-1}$  yield  $\delta$ -crystals that subsequently convert to triclinic  $\alpha$ -crystals upon solidification.<sup>8</sup>

We first determined the cooling rate for PA11 in an injection-molded tensile bar by simulating flow and thermal transfer using Autodesk Moldflow 2016.<sup>14</sup> We tracked the flow and transfer at depths of 50, 200, 700, and  $1000\mu\text{m}$  at specific locations, as shown in Figure 1. We recorded the cooling rate profiles obtained for each node from high to low temperatures as the melt cools in simulation, ending when the melt reaches the same temperature as the mold. Heat transfer varies with the distance from the mold steel, so each of these nodes cools at a different rate. Figure 2 shows the cooling rate profiles for each node as green, red, white, and blue data points at mold temperatures of 25, 50, and  $80^\circ\text{C}$ .

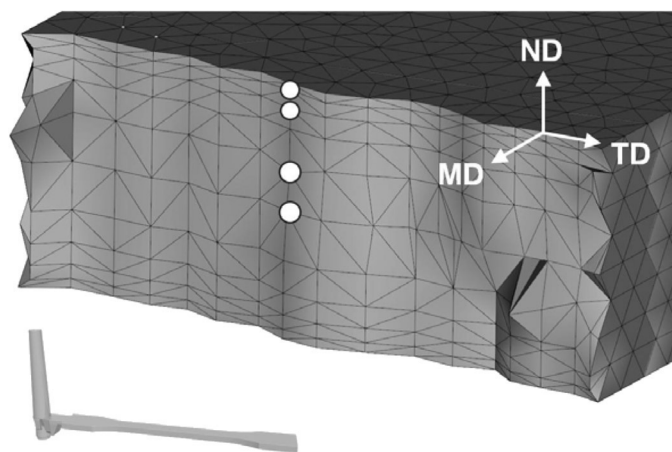


**Figure 1.** CAD 3D model (main image) of the molded polyamide 11 (PA11) specimen (inset bottom left) imported to Moldflow software and locations assigned for the simulation (white spots, top) at distances of 50, 200, 700, and  $1000\mu\text{m}$  from the surface. MD, ND, TD: Melt flow direction, normal to melt flow direction, and transverse to melt flow direction, respectively.

The stars in Figure 2 show cooling rate crystallization data from a previous study: as the cooling rate of PA11 increases, the crystallization temperature decreases.<sup>9</sup> The green, red, and blue dashed lines in Figure 2 show the temperatures at which the stars intersect with the simulated cooling rate profiles and hence the temperature at which our simulated cooling profiles predict the polymer will actually crystallize. For mold temperatures of 25, 50, and  $80^\circ\text{C}$ , crystallization occurs at  $117\text{--}135$ ,  $123\text{--}139$ , and  $131\text{--}142^\circ\text{C}$ , respectively.

To evaluate this approach, we molded physical samples under the same conditions as those studied in simulation. Tensile bars of PA11 from each mold temperature of interest were then sectioned and characterized using wide-angle x-ray diffraction (XRD).

Using XRD, we identified the specific crystalline polymorph ( $\alpha$ ,  $\delta$ , or  $\delta'$ ) at each location. For brevity, we describe only the  $50^\circ\text{C}$  mold temperature sample in detail. At depths of 50 and  $700\mu\text{m}$ , we expect (from the data in Figure 2) that the polymer will crystallize at  $121$  and  $139^\circ\text{C}$ ,

*Continued on next page*

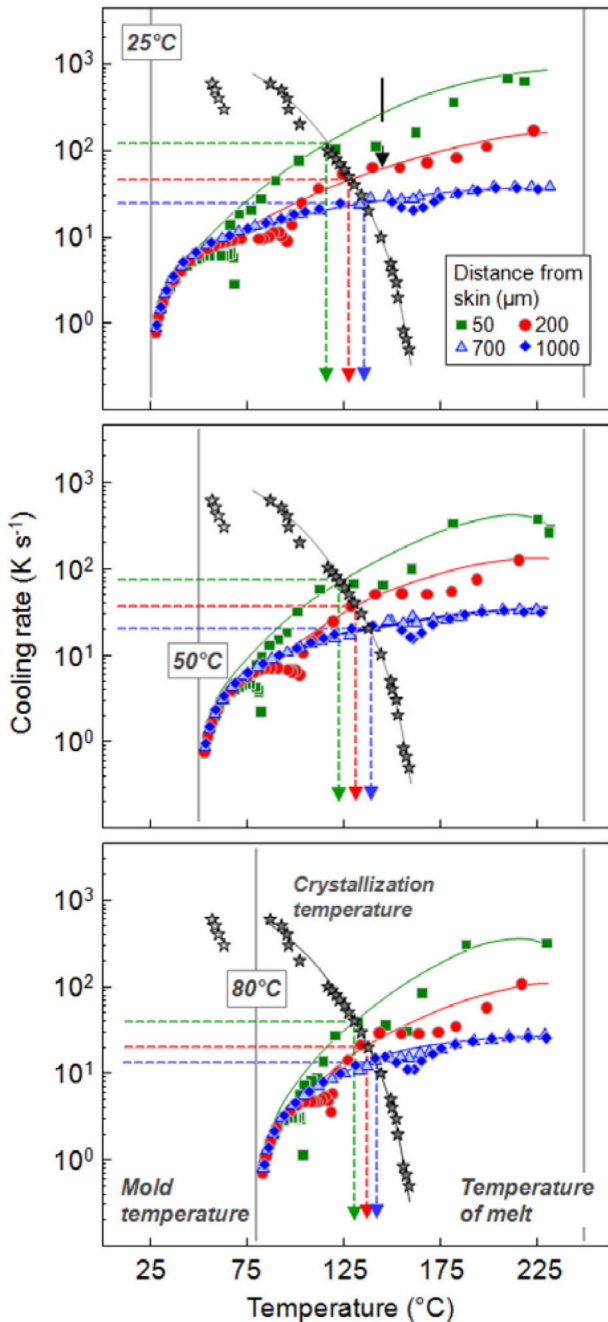


**Figure 2.** Simulated cooling rates during injection molding of PA11 at different distances from the mold wall shown by green (50 $\mu\text{m}$ ), red (200 $\mu\text{m}$ ), white (700 $\mu\text{m}$ ), and blue (1000 $\mu\text{m}$ ) symbols and lines for mold temperatures of 25 (top), 50 (middle), and 80 $^{\circ}\text{C}$  (bottom). The star symbols in each plot show temperatures of crystallization of PA11, which were measured as a function of cooling rate in a separate study.<sup>9</sup>

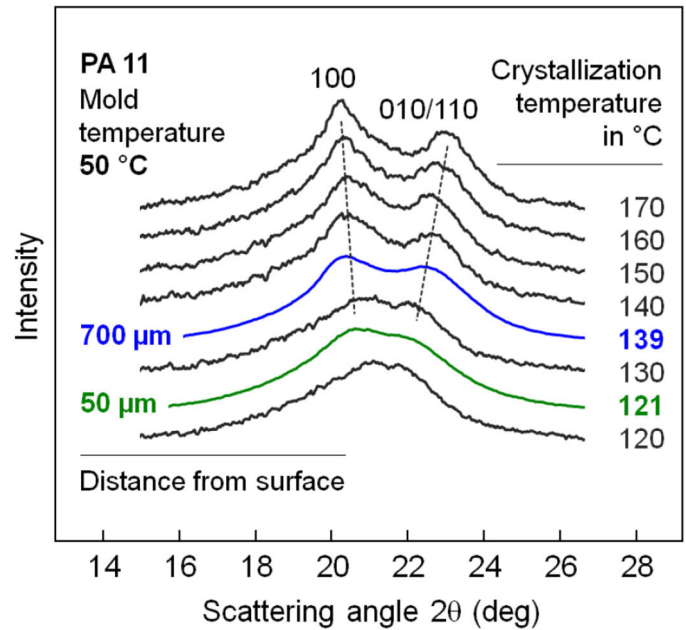


**Figure 3.** X-ray diffraction patterns of PA11 moldings prepared with a mold temperature of 50 $^{\circ}\text{C}$  taken at different distances from the surface of the 50 $\mu\text{m}$  (green) and 700 $\mu\text{m}$  (blue) fit well into a series of patterns for isothermally prepared PA11 of the same grade sorted by crystallization temperature.

respectively. If so, then XRD data should prove similar between the molded sample and a sample of the same material isothermally crystallized from a pellet. This is indeed the case. Figure 3 shows that XRD patterns from samples extracted from the molded bar (blue and green lines) fit well into a series of XRD patterns of isothermally prepared PA11 samples sorted by crystallization temperature. Other results indicate that the quality of the  $\alpha$ -crystal increases with sample depth and also with increasing mold temperature, in both cases due to longer cooling times.

In summary, we have shown the link between traditional isothermal calorimetric studies and the molded microstructure obtained in practice. Although we did not consider the influence of shear effects or flow-induced crystallization, our predictions are nevertheless in striking agreement with isothermal analysis. This indicates that, at least for this grade of PA11 under these processing conditions, thermal effects dominate the crystallization process. It is in principle possible to predict the aggregate microstructure and hence bulk properties of processed PA11. Ongoing studies address the non-isothermal crystallization of this polymer after melt flow.

Financial support by the Deutsche Forschungsgemeinschaft (DFG) (grant AN 212/18) is gratefully acknowledged. The authors are thankful to Nichole Wonderling (Materials Characterization Laboratory, Penn State) for assistance in x-ray data collection.

## Author Information

### Katalee Jariyavidyanont and René Androsch

Martin Luther University Halle-Wittenberg  
Halle (Saale), Germany

### Jason L. Williams and Alicyn M. Rhoades

Plastics Engineering Technology  
Penn State Behrend  
Erie, PA

Alicyn Rhoades is an assistant professor and leads research focused on process-induced microstructure development in polymers.

### Ines Kühnert

Institute of Polymer Materials  
Dresden, Germany

### Walter Focke

Department of Chemical Engineering  
University of Pretoria  
Pretoria, South Africa

## References

1. R. Aelion, *Structure of nylon 11*, **Annali di Chimica Applicata** **3** (5-61), p. 565, 1948.
2. K. G. Kim, B. A. Newman, and J. I. Scheinbeim, *Temperature dependence of the crystal structures of nylon 11*, **J. Polym. Sci. B: Polym. Phys.** **23** (12), pp. 2477–2482, 1985. doi:10.1002/pol.1985.180231206
3. P. K. Chen, B. A. Newman, J. I. Scheinbeim, and K. D. Pae, *High pressure melting and crystallization of Nylon-11*, **J. Mater. Sci.** **20** (5), pp. 1753–1762, 1985. doi:10.1007/BF00555281
4. B. A. Newman, T. P. Sham, and K. D. Pae, *A high-pressure x-ray study of Nylon 11*, **J. Appl. Phys.** **48** (9), pp. 4092–4098, 1977. doi:10.1063/1.323435
5. S. Gogolewski, *Effect of annealing on thermal properties and crystalline structure of polyamides. Nylon 11 (polyundecaneamide)*, **Colloid Polym. Sci.** **257** (8), pp. 811–819, 1979. doi:10.1007/BF01383352
6. Q. Zhang, Z. Mo, H. Zhang, S. Liu, and S. Z. D. Cheng, *Crystal transitions of Nylon 11 under drawing and annealing*, **Polymer** **42** (13), pp. 5543–5547, 2001. doi:10.1016/S0032-3861(01)00050-7
7. S. S. Nair, C. Ramesh, and K. Tashiro, *Polymorphism in Nylon-11: characterization using HTWAXS and HTFTIR*, **Macromol. Symp.** **242**, pp. 216–226, 2006. doi:10.1002/masy.200651030
8. L. J. Mathias, D. G. Powell, J. P. Autran, and R. S. Porter, *Nitrogen-15 NMR characterization of multiple crystal forms and phase transitions in polyundecanamide (Nylon 11)*, **Macromolecules** **23**, pp. 963–967, 1990.
9. A. M. Rhoades, N. Wonderling, C. Schick, and R. Androsch, *Supercooling-controlled heterogeneous and homogenous crystal nucleation of polyamide 11 and its effect onto the crystal/mesophase polymorphism*, **Polymer** **106**, pp. 29–34, 2016. doi:10.1016/j.polymer.2016.10.050
10. R. Brill, *Über das Verhalten von Polyamiden beim Erhitzen*, **J. Prakt. Chem.** **161**, pp. 49–64, 1942.
11. G. F. Schmidt and H. A. Stuart, *Gitterstrukturen mit räumlichen Wasserstoffbrückensystemen und Gitterumwandlungen bei Polyamiden*, **Z. Naturforsch.** **13a**, pp. 222–225, 1958.
12. K. Jariyavidyanont, J. L. Williams, A. M. Rhoades, I. Kühnert, W. Focke, and R. Androsch, *Crystallization of polyamide 11 during injection molding*, **Polym. Eng. Sci.**, 2017. doi:10.1002/pen.24665
13. A. Mollova, R. Androsch, D. Mileva, C. Schick, and A. Benhamida, *Effect of supercooling on crystallization of polyamide 11*, **Macromol.** **46**, pp. 828–835, 2013.
14. <https://www.autodesk.com/campaigns/moldflow2016> Autodesk website. Accessed 2 March 2018.